

# The Influence of Surface Donor States on the Chemisorption Kinetics of Oxygen at the Surface of ZnO Single Crystals

## II. Experimental Results

E. ARIJS\*, F. CARDON, AND W. MAENHOUT-VAN DER VORST

*Laboratorium voor Kristallografie en Studie van de Vaste Stof, Krijgslaan, 271, B-9000 Gent, Belgium*

Received March 14, 1972

A kinetic study was performed of the conductivity changes in Li-doped ZnO single crystals due to the adsorption of oxygen, after illumination of the surface in vacuum. The influence of the oxygen pressure and of the previous illumination have been studied. The results suggest that: (i) the chemisorption kinetics can be explained, over a wide range of conductivities, by a model, which involves an accumulation layer; (ii) the accumulation layer originates from the presence of surface donor states, whose density can be varied by illumination in vacuum; (iii) the rate-limiting step of the process is the capture of the electron in the physisorbed species; (iv) the surface concentration of the physically adsorbed oxygen is directly proportional to the pressure.

### 1. Introduction

During the past two decades, the adsorption of oxygen on ZnO has been extensively studied by conductivity measurements (1). The kinetics of the adsorption process have generally been represented by means of an Elovich rate equation (2-4).

In these studies the oxygen adsorption has been investigated on sintered layers (3-5) or on single crystals (4) after illumination of the specimens in neutral gas flows or in vacua of the order of  $10^{-6}$  Torr. The result of the illumination cycle was interpreted as a desorption of the previously adsorbed oxygen. The observed conductivity changes, however, were relatively small.

In the present work the oxygen adsorption kinetics are investigated on ZnO single crystals after a long illumination cycle in ultra high vacuum ( $10^{-8}$  to  $10^{-9}$  Torr). In order to avoid the difficulties inherent to thin specimens, Li-doped single crystals have been used. Conductivity changes over several orders of magnitude have been observed.

Furthermore a detailed study of the pressure

\* Present address: Belgisch Instituut voor Ruimte-aëronomie, Ringlaan 3, B-1180 Brussels, Belgium.

dependence of the adsorption kinetics is presented. From this it is concluded that the density of the physically adsorbed oxygen is directly proportional to the ambient pressure.

The results of the experiments are shown to support the theoretical model derived in paper I (6).

### 2. Experimental Methods

Two types of crystals have been used in our experiments:

1. Li-doped ZnO wafers purchased from the 3-M Company.

2. Pure vapor phase grown crystals obtained from the "Institut für Angewandte Physik" of the university of Erlangen (Germany). All crystals had a thickness of about 0.5 mm and a diameter of  $\pm 5$  mm. The pure crystals were doped by a method similar to the one described by Lander (7). After polishing, the crystals were chemically etched with 11 M HCl (20 sec) and polished with 85%  $H_3PO_4$  (1 hr). In order to avoid surface conductivity due to etching (8) the crystals were heated afterwards at 300°C during 10 min in air.

The specimens were then provided with ohmic indium contacts so that the current flow was parallel to the (000I) surface, which was identified by the etch pattern (9, 10). The samples were mounted in a stainless steel cell with suitable provisions for the electrical leads and illumination. The measuring cell could be evacuated down to  $10^{-8}$  Torr after a bake out at  $140^{\circ}\text{C}$ . In order to avoid the Indium contact from melting during the bake-out, a good temperature control of the specimen was necessary. This was achieved by mounting the crystals on thin BeO platelets, which were attached to a copper block. At the same time excessive heating of the sample during intense illumination was avoided in this way. Irradiation of the sample was performed by a 150 W Xe arc (Bausch and Lomb), the intensity of which could be varied by the use of grey filters (Balzers). The sample current was measured with a Keithley 610 B electrometer, the output of which was connected to a pen recorder. The voltage across the sample was supplied by a battery.

After mounting and bake-out, the samples were illuminated at the highest light intensity, during three hours, in vacuum. Oxygen was then introduced into the measuring cell at a pressure of 45 cm Hg, and the conductivity was allowed to decay during at least 4 hr. After this treatment,

which is referred to as a cleaning cycle, the room temperature dark resistivity always exceeded  $10^{10}$  ohm cm. After this cleaning cycle the cell was evacuated again to  $3 \times 10^{-8}$  Torr, without a bake-out. The measurements were then started and consisted of:

a. illumination of the sample in vacuum with suitable light intensity during a given period  $(\Delta t)_L$ ; during which the conductivity increased over several orders of magnitude to a value  $G_L$ .

b. turning off the light and allowing the conductivity to decay to a value  $G_a$ , corresponding to a normalized resistance  $R_{na}$ . The normalized resistance  $R_n$  is defined by  $R_n = R b/l$  ( $b$  being the width of the specimen and  $l$  the distance between the electrodes), according to our previous work (11).

c. introduction of oxygen in the cell at a pressure  $p_{o_2}$ . This accelerates the conductivity decay spectacularly. The normalized resistance is then recorded as a function of time. The pressure was measured with an open Hg manometer, which could be isolated from the cell during the high vacuum cycle.

d. reevacuation of the cell. During this procedure the conductivity remains practically unchanged. Small changes are observed, which may be due to the adsorption of activated oxygen, originating from the vacuum pump.

TABLE I  
VALUES OF THE PARAMETERS CORRESPONDING TO THE CURVES OF FIGS. 1, 2, AND 3

Expt no.	Sample	Curve no.	Illumination		$R_{na} (\Omega)$	$(\Delta t)_D$	$p_{o_2}$ (mm Hg)	$t_b$ (sec)	$R_{nb} (\Omega)$
			Relative intensity (%)	Period $(\Delta t)_L$ (sec)					
I (Fig. 1)	A (Erlangen)	1	5.2	3720	$9.25 \times 10^5$	850	390	20	$2.11 \times 10^7$
		2		5220	$2.81 \times 10^6$	1540	389		$3.47 \times 10^7$
		3		1740	$1.26 \times 10^7$	600	391		$7.61 \times 10^7$
		4		1140	$2.76 \times 10^7$	—	391		$3.38 \times 10^8$
		5		480	$9.35 \times 10^7$	600	391		$9.97 \times 10^8$
		6		300	$2.64 \times 10^8$	690	389		$2.33 \times 10^9$
		7		100	$9.86 \times 10^8$	240	391		$5.94 \times 10^9$
II (Fig. 2)	B (3M-Co)	8	2.5	1980	$1.91 \times 10^7$	1270	410	100	$1.44 \times 10^9$
		9		2580	$1.91 \times 10^7$	1750	150		$6.66 \times 10^8$
		10		2940	$1.95 \times 10^7$	1800	75		$3.18 \times 10^8$
		11		6600	$1.91 \times 10^7$	3400	36		$1.85 \times 10^8$
III (Fig. 3)	B	12	4.7	2700	$1.91 \times 10^7$	1240	18	100	$1.78 \times 10^8$
		13		4080	$1.91 \times 10^7$	2200	18		$1.22 \times 10^8$

### 3. Results

The experimental data were obtained on two single crystals. Sample A is a crystal obtained from the University of Erlangen and sample B is purchased from the 3-M Company. These results are representative for the data obtained on other crystals, prepared in the same way.

The parameters, which can be varied experimentally in order to study the chemisorption process are: the time of illumination ( $\Delta t$ )<sub>L</sub>, the relative intensity of illumination, the time of decay after illumination in vacuum ( $\Delta t$ )<sub>D</sub>, and the oxygen pressure  $p_{O_2}$ . The values of these parameters are summarized in Table I, for the different experiments.

The conductivity decay during oxygen adsorption is plotted as  $\log(R_n - R_{nb})$  versus  $\log(t - t_b)$ . It was assumed that the gas was homogeneously distributed in the cell from a time  $t_b$  on, depending upon the gas pressure. The value of  $R_n$  corresponding to the time  $t_b$  is denoted by  $R_{nb}$ .

In Expt. I the intensity of illumination has been kept constant and the illumination time has been varied in order to obtain different values of  $R_{na}$ . The adsorption kinetics have then been studied at a fixed oxygen pressure. The results are shown in Fig. 1.

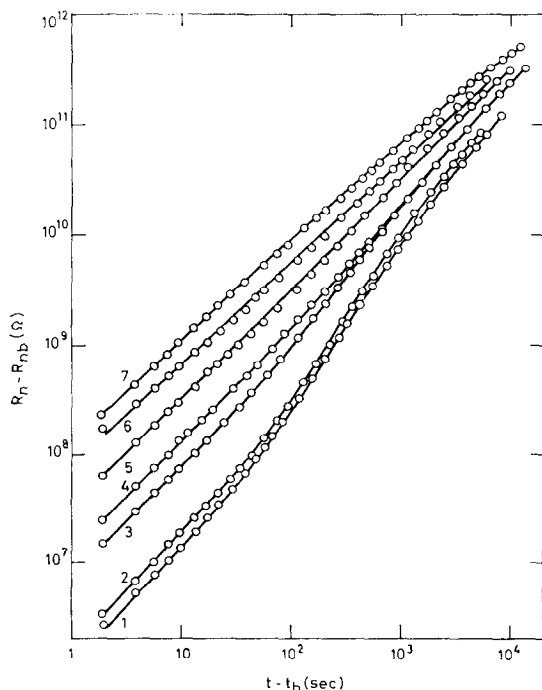


FIG. 1.  $R_n - R_{nb}$  versus  $t$ , during oxygen adsorption for different  $R_{na}$  values.

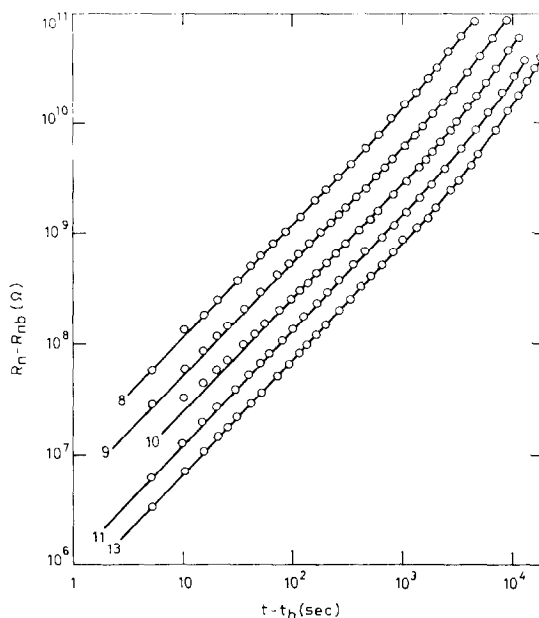


FIG. 2.  $R_n - R_{nb}$  versus  $t$ , during oxygen adsorption for different oxygen pressures.

In Expt. II the influence of the oxygen pressure on the adsorption kinetics has been studied at a fixed value of  $R_{na}$ .

In order to obtain identical  $R_{na}$  values, the sample has always been illuminated with the same light intensity to the same conductivity level  $G_L$ .

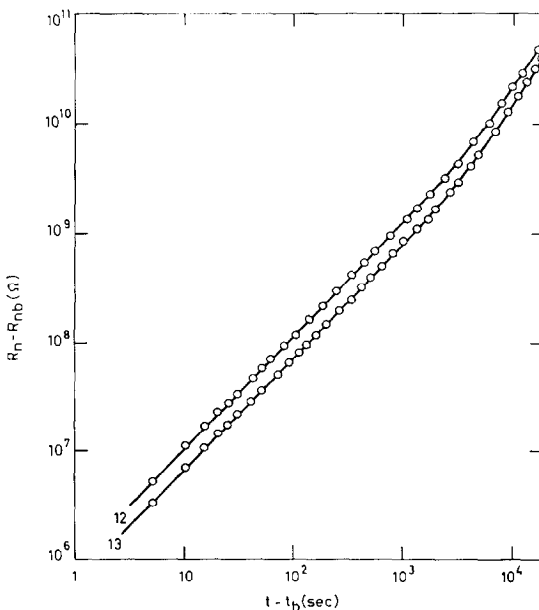


FIG. 3.  $R_n - R_{nb}$  versus  $t$ , during oxygen adsorption for different previous illuminations.

The corresponding adsorption kinetics are shown in Fig. 2. It can be seen from Table I that in Expt. II the time  $(\Delta t)_L$ , needed to obtain the same  $G_L$  level increases for successive cycles.

The influence of the illumination intensity was investigated in Expt III. In this experiment the equal  $R_{na}$  values have been obtained after decay from the same value of  $G_L$  to the same value of  $G_a$ . The conductivity  $G_L$  had been reached with different light intensities. As shown in Fig. 3, the  $\log(R_n - R_{nb})$  versus  $\log(t - t_b)$  curves do not coincide.

#### 4. Discussion

##### 4.1. The Existence of Surface Donor States

It must be emphasized that the conductivity change, due to illumination in vacuum can be completely reversed by oxygen adsorption. Assuming this effect to be due, during irradiation, to the annihilation of a depletion layer, and the subsequent formation of such a layer, during oxygen adsorption, the thickness of this space charge layer should be of the order of magnitude of half the thickness of the crystal ( $W/2$ ). For a Schottky barrier the height  $V_s$  would thus be given by:

$$V_s = \frac{2\pi}{\epsilon} \cdot e(W/2)^2 n_0, \quad (1)$$

$n_0$  being the effective bulk donor density. Assuming a reasonable upper limit of 0.5 V for  $V_s$  and inserting the appropriate value for  $\epsilon$  of 8.5 (12) one finds for crystal B ( $W = 0.38$  mm) a value of  $n_0$  of  $1.3 \times 10^{10}$  cm $^{-3}$ , which corresponds to  $R_n = 7 \times 10^7 \Omega$ . As shown in Table I,  $R_{na}$  is smaller than this value. Therefore it is reasonable to accept that an accumulation layer is present at the surface at the moment of oxygen inlet. The existence of the accumulation layer may be due to surface states created by photolysis during the illumination of the crystals in vacuum (13, 14).

The influence of such donor states on the adsorption kinetics has been theoretically studied in paper I (6). The results of this model are now compared to the experimental data.

##### 4.2. Influence of the Surface Donor State Density on the Chemisorption Kinetics

In paper I (6) it has been shown that a relationship of the form,

$$R_n - R_{nb} = \eta t, \quad (2)$$

is valid in four cases. On log-log plot, Eq. (2) results in a straight line with slope 1. Such a

relationship is observed over several orders of magnitude for moderate values of  $R_{na}$  as can be seen from Table I and Figs. 2 and 1 (curves 4 and 5). For smaller values of  $R_{na}$ , the relationship, representing the conductivity changes due to oxygen adsorption, becomes more complicated, as is illustrated by curves 1, 2 and 3 of Fig. 1. Curves of this form have been predicted in the theory for high density of surface donors  $N_s$ , which corresponds to large band bending.

From the formula

$$R_{na} = \frac{1}{e\mu W} \frac{1}{[n_0 + (2/W)(N_s^+ - N_0^-)]}, \quad (3)$$

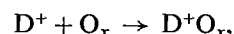
where  $N_s^+$  and  $N_0^-$  are the densities of ionized surface donors and chemisorbed oxygen, respectively, it can be seen that high values of  $N_s$  which implicates high values of  $N_s^+$  correspond to low values of  $R_{na}$ . For the curves 1 to 5 a good qualitative agreement is noticed with the theory.

The increase of surface donor state density with increasing illumination time can be explained by further photolysis of the ZnO surface.

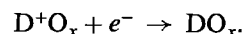
For higher values of  $R_{na}$ , deviations from the linear  $R_n - R_{nb}$  versus  $t$  relationship are observed for higher  $t$  values, as is shown by curves 6 and 7 of Fig. 1. Since, however the effective bulk donor density of our samples is not known, it is not possible to point out which of the four cases, where Eq. (2) may be applied, must be considered. Therefore the results of curve 6 and 7 cannot be considered as being in disagreement with the theory.

In paper I (6) it has been assumed that no interaction occurs between the surface donors and the adsorbed oxygen species. One can imagine two kinds of interaction, such that the model presented in paper I (6) loses its validity. These are

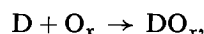
a. The transition from physisorbed oxygen to chemisorbed oxygen happens at the ionized surface donors, according to the reactions



where  $D^+$  represents an ionized donor and  $O_x$  a physisorbed oxygen specie ( $x = 1$  or  $2$ ), and



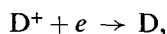
b. Chemisorption occurs at the nonionized surface donors



where  $D$  stands for a nonionized donor. In this case the oxygen is chemically bound to the semi-

conductor surface by the electron of the non-ionized donor. Such a reaction lowers the total number of surface donors (as well as the foregoing one).

The conductivity changes in the latter case are the result of the charge redistribution in the remaining donors according to the reaction



where the electron is taken from the conduction band. In this case the normalized resistivity  $R_n$  of the crystal would at any moment be given by

$$R_n = \frac{1}{e\mu W} \frac{1}{[n_0 + (2N/W)]},$$

where  $N = N_s^+$ . This implies that all points from Fig. 1 with equal  $R_n$  values (which are situated on different curves) would be characterized by the same physical situation.

Since the oxygen pressure is the same for all curves of Fig. 1 we can expect to find curve 4 if we redraw curve 1 by choosing  $t_b'$  given by

$$R_{nb}(t_b') = R_{nb}(4) = 3.4 \times 10^8 \Omega,$$

where  $R_{nb}(4)$  is the value of  $R_n$  at  $t = t_b$  for curve 4. This has been done in Fig. 4 for four points of

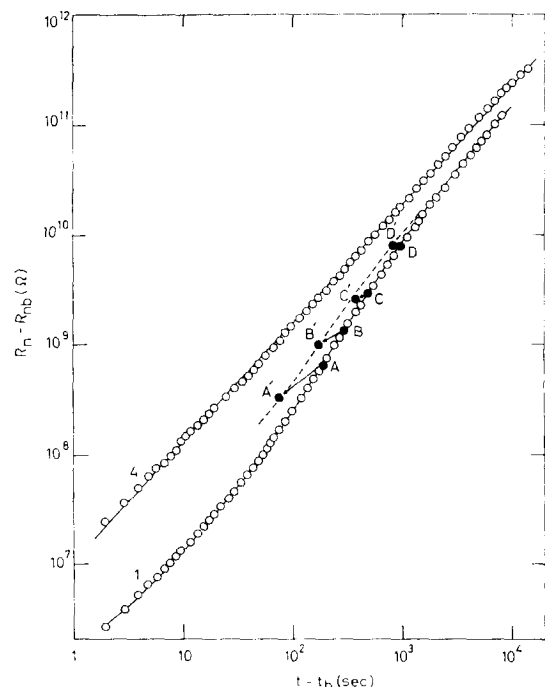


FIG. 4. Comparison of the resistivity rise during oxygen adsorption at the same  $R_{nb}$  values corresponding to different surface coverages.

curve 1. We notice that the obtained new curve does not coincide with curve 4 (and even has a quite different form). Therefore it can be concluded that the interaction of the adsorbed oxygen with the nonionized surface donors cannot be dominant.

It is shown in the Appendix that if the interaction of ionized surface donors with the adsorbed oxygen is important the observed behavior of the resistance as a function of time cannot be explained.

#### 4.3. Pressure Dependence of the Chemisorption Kinetics

If  $R_n - R_{nb}$  increases linearly with time the coefficient  $\eta$  is proportional to the density of physisorbed oxygen  $N_0$ . Since, from the data of Fig. 2  $\eta$  can be obtained at different values of the oxygen pressure, the pressure dependence of  $N_0$  can, in principle, be derived from the curves of Fig. 2. Care however must be taken by applying this procedure, since the linear relationship can be found the following four cases:

a. The Debye length  $L_D$  is larger than the thickness of the crystal. Here we distinguish three possibilities.

i. The conductivity due to the surface donors is larger than the conductivity due to volume donors. In this case  $\eta$  is directly proportional to the density of physisorbed oxygen  $N_0$  and with a number of constants independent of the measuring conditions.

ii. The conductivity due to surface donors can be neglected with regard to the volume conductivity, though an accumulation layer is still present at the surface. In this case  $\eta \sim n_0 N_0 R_{nb}^2$ .

iii. A depletion layer is present at the surface at the moment of oxygen inlet. For small values of  $t$  Eq. (2) is still valuable and  $\eta \sim R_{nb} N_0$ .

b. The volume donors are partly compensated and  $L_D \ll W$ . In this case Eq. (2) is only valuable in a small range of  $t$  values (6). Since in Fig. 2 Eq. (2) is valuable over several orders of magnitude this last case can be excluded.

In order to investigate which of the first 3 cases is valuable for Fig. 2 curve 13 has been redrawn for different  $R_{nb}$  values and  $\eta$  has been plotted versus  $R_{nb}$  in Fig. 5. It can be seen that as long as  $R_{nb} < 7 \times 10^8 \Omega$   $\eta$  is independent of  $R_{nb}$ . In a similar way it can be shown that for all curves of Fig. 2  $\eta \sim N_0$ .

From the curves 8 to 11 and curve 13 the values of  $\eta$  at different oxygen pressures have

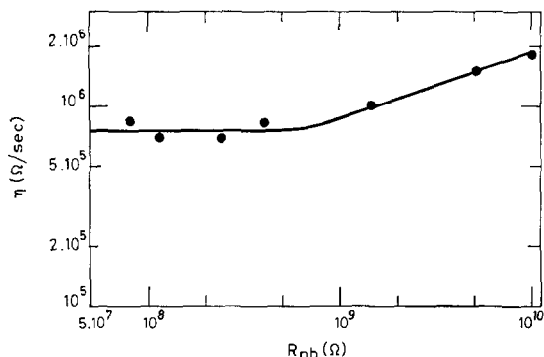


FIG. 5.  $\eta$  as a function of  $R_{nb}$ .

been obtained and are plotted in Fig. 6. The value of cycle 12 has been omitted in this graph. The reason for this is discussed below.

By applying a linear regression analysis to these points it can be shown that

$$\log \eta (\Omega/\text{sec}) = 4.5 + 1.001 \log p \text{ (mm)},$$

with a correlation coefficient of 0.996. This indicates that  $\eta \sim p$ . Since in this case  $\eta \sim N_0$ , we can conclude that  $N_0 \sim p$ . In other words, a linear relation between the density of the physisorbed oxygen and the pressure has been found, in the pressure ranges considered here. The existence of  $O_2^-$  has been shown by ESR measurements on the ZnO- $O_2$  system (15, 16). The experiments, described above, thus suggest that the process, which is responsible for the electron capture during oxygen chemisorption is the reaction  $(O_2)_s + e \rightarrow (O_2^-)_s$ .

It must be pointed out that in order to find the linear dependence of  $\eta$  on  $p$ , the  $R_{na}$  values of Fig. 2 must not only have the same value but must also be reached in the same way. This is

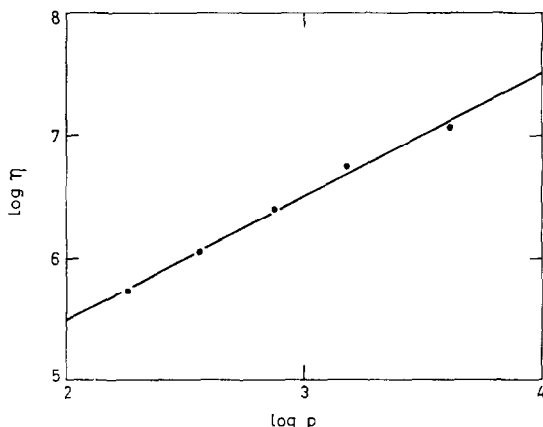


FIG. 6. Pressure dependence of  $\eta$ .

illustrated in Expt III, where  $R_{na}$  is obtained by illuminating with the double light intensity and where all other parameters have been kept constant. The different  $\eta$  values calculated from Fig. 3 indicate that  $\eta$  is a function of the previous illumination intensity. Therefore the  $\eta$  value of curve 12 has been omitted in Fig. 6. The fact that  $\eta$  is a function of the previous illumination intensity suggests that  $N_0$  is also dependent upon the illumination. Such memory effects have been recently described by Wolkenstein and Baru (17). A similar explanation is probably to be expected in our case, however more experimental facts are necessary to elucidate this problem.

#### 4.4. The Dark Conductivity for Flat Energy Bands

According to the model described in paper I (6) it is stated that as long as  $\eta$  is not influenced by the value of  $R_{nb}$

$$N_B \geq n_0 \frac{W}{2} \quad \text{or} \quad \frac{1}{2} R_{n0} \geq (R_{nb})_g,$$

where  $R_{n0}$  is the normalized resistance at flat energy bands and  $(R_{nb})_g$  is the maximum value of  $R_{nb}$  where  $\eta$  is still independent of  $R_{nb}$ .

From Fig. 5 it follows that

$$R_{n0} \geq 1.4 \times 10^9 \Omega.$$

Since  $R_{n0} = (e\mu W n_0)^{-1}$  and  $W \cong 0.4$  mm we find

$$n_0 \leq 6 \times 10^8 \text{ cm}^{-3}.$$

On the other hand it has been shown in paper I (6) that for

$$N < \frac{\epsilon k T}{2\pi e^2 W} \quad \text{or} \quad N < 6 \times 10^6 \text{ cm}^{-2},$$

Eq. (2) is no longer valid, which means that for

$$R_n > \frac{1}{e\mu W} \times \frac{1}{n_0 + (2/W)(\epsilon k T / 2\pi e^2)(1/W)},$$

deviations from the linear  $R_n - R_{nb}$  versus  $t$  relationship should occur. With  $n_0 \leq 6 \times 10^8 \text{ cm}^{-3}$  this limit value is:

$$R_n \geq 10^9 \Omega.$$

This is in good agreement with the observed kinetics in Fig. 5, which supports the model proposed in paper I (6).

## 5. Conclusions

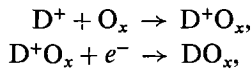
From the discussion it follows that a good qualitative agreement between the proposed model (6) and the experimental data is found.

An exact quantitative analysis of the experimental data is not possible at this stage. The model must probably be refined before a complete accurate fitting of the experimental results to the theory can be exposed.

In spite of all the assumptions made (6), the qualitative agreement over several orders of magnitude in time is very satisfactory, which proves the basic ideas of the model to be exact.

## 6. Appendix

In this section we give a concise deviation of the chemisorption kinetics if the following reactions occur



with the symbols defined in paper I (6) and at the end of this section, the set of equations defining the chemisorption kinetics are

$$\begin{aligned} N_S &= N_S^+ + N_S^0 + N_0 + N_0^-, \\ N_0 &= k_1 N_S^+, \\ N_S^+ &= f(N_S^+ + N_S^0), \\ 1/f &= 1 + \frac{n_s}{N_c} \exp \frac{E_S}{kT}, \\ N &= N_S^+ + N_0, \\ \frac{dN_0^-}{dt} &= uS_n' \cdot n_s N_0. \end{aligned}$$

Elimination leads to

$$\begin{aligned} \left[ 1 + \frac{1}{k_1} + \frac{n_s}{k_1 N_c} \exp \frac{E_S}{kT} \right] \frac{dN}{dt} \\ + \frac{N}{k_1 N_c} \exp \frac{E_S}{kT} \cdot \frac{dn_s}{dt} = -uS_n' n_s N'. \end{aligned} \quad (4)$$

This differential equation can be integrated by putting either

$$n_s = \frac{2\pi e^2}{\epsilon kT} \cdot N^2,$$

for large accumulation, or

$$n_s = n_0 + \frac{2N}{W},$$

for small accumulation.

In the first case one finds, after transition to  $R_n$  through the formula

$$\begin{aligned} R_n &= \frac{1}{e\mu W N}, \\ \left[ 1 + \frac{1}{k_1} \right] (e\mu)^2 (R_n^2 - R_{nb}^2) \\ + \frac{3\pi e^2}{\epsilon kT} \frac{1}{k_1 N_c} \exp \frac{E_S}{kT} \ln \frac{R_n}{R_{nb}} &= \frac{\pi e^2}{\epsilon kT} \cdot uS_n' t. \end{aligned}$$

This expression cannot explain the experimental results for high accumulation, which corresponds to low resistance.

By putting  $n_s = n_0 + (2N/W)$  Eq. (4) can again be integrated, but the resulting equation

$$\begin{aligned} a_2 \ln \frac{N}{N + n_0(W/2)} + b_2 \ln \left( N + n_0 \frac{W}{2} \right) \\ = -c_2 t + A, \end{aligned}$$

where

$$\begin{aligned} a_2 &= 1 + \frac{1}{k_1} + \frac{n_0}{k_1 N_c} \exp \frac{E_S}{kT}, \\ b_2 &= \frac{2n_0}{W} \frac{1}{k_1 N_c} \exp \frac{E_S}{kT}, \\ c_2 &= uS_n' \cdot n_0, \end{aligned}$$

and  $A$  is an integration constant does not fit the experimental results neither.

### List of New Symbols Used in the Appendix

$N_S$	total number of surface donors/cm <sup>2</sup>
$N_S^+$	density of ionized surface donors ( $D^+$ )
$N_S^0$	density of neutral surface donors
$N_0$	density of physisorbed oxygen (product $D^+O_x$ )
$N_0^-$	density of chemisorbed oxygen (product $DO_x$ )

### Acknowledgments

The authors are very indebted to Professor Dr. W. Dekeyer for his continuous interest in this work. They also thank Dr. R. Helbig of the Institut für Angewandte Physik at the University of Erlangen for providing some of the single crystals used in this work.

### References

1. G. HEILAND, E. MOLLWO, AND F. STÖCKMAN in "Solid State Physics" (E. Ehrenreich, F. Seitz and D. Turnbull, Eds.), Vol. 8, p. 193-296, Academic Press, New York, 1959.
2. D. B. MEDVED, *J. Chem. Phys.* **28**, 870 (1958).
3. D. A. MELNICK, *J. Chem. Phys.* **26**, 1136 (1957).
4. H. J. VAN HOVE AND A. LUYCKX, *Solid State Commun.* **4**, 603 (1966).
5. D. B. MEDVED, *J. Phys. Chem. Solids* **20**, 255 (1961).
6. E. ARIJS AND F. CARDON, *J. Solid State Chem.* **6**, 310 (1973).
7. J. J. LANDER, *J. Phys. Chem. Solids* **15**, 324 (1960).
8. W. WEGENER, Diplomarbeit, Aachen, 1967.
9. A. R. MARIANO AND R. E. HANNEMAN, *J. Appl. Phys.* **34**, 384 (1963).

10. G. HEILAND, P. KUNSTMANN, AND H. PFISTER, *Z. Phys.* **176**, 485 (1963).
11. E. ARIJS, F. CARDON, AND W. MAENHOUT-VAN DER VORST, *Surface Sci.* **17**, 387 (1969).
12. A. R. HUTSON, *Phys. Rev.* **198**, 222 (1957).
13. R. J. COLLINS AND D. G. THOMAS, *Phys. Rev.* **112**, 388 (1958).
14. S. R. MORRISON, *J. Vac. Sci. Technol.* **7**, 84 (1970).
15. K. M. SAUCIER, *J. Catal.* **5**, 314 (1966).
16. R. D. IYENGAR, V. V. SUBA RAO, AND A. C. ZETTMAYER, *Surface Sci.* **13**, 251 (1969).
17. T. WOLKENSTEIN AND V. BARU, *Surface Sci.* **13**, 294 (1969).